

Impact of Communication Erasure Channels on Safety of Highway Vehicle Platoons

Lijian Xu, *Member, IEEE*, Le Yi Wang, *Fellow, IEEE*, George Yin, *Fellow, IEEE*, Hongwei Zhang, *Senior Member, IEEE*,

Abstract—Packet loss in block erasure channels creates a randomly switching networked system that impacts control performance significantly. This paper employs safety of highway vehicle platoons as a platform to study such an impact. By autonomous inter-vehicle coordination, a platoon can potentially enhance safety, improve highway utility, increase fuel economy, and reduce emission. By comparing different information structures which utilize radar distance sensors and wireless communication channels, we characterize some intrinsic relationships between communication resources and control performance. The findings of this paper provide useful guidelines in communication resource allocations and vehicle coordination in vehicle safety problems.

Index Terms—Highway platoon, communications, vehicle safety, erasure channels, control.

I. INTRODUCTION

Platoon formation has been identified as a promising framework in developing intelligent transportation systems. Wireless communication systems can provide inter-vehicle information that is of potential importance in enhancing safety, improving highway utility, increasing fuel economy, and reducing emission. In platoon formation and maintenance, distributed supervisors in vehicles adjust vehicle spatial distributions based on inter-vehicle information via sensors and wireless communication networks such that roadway utilization is maximized while the risk of collision is minimized or avoided.

Platoon control has been studied as part of intelligent and automated highway systems with various control methodologies and demonstration systems, including the California PATH project and European Chauffeur systems in the 1980's, and more recent DEMO2000, CarTALK2000, FleetNet, AHS and SARTRE [1], [2], [3], [4], [5], [6], [7]. In our recent paper [8], a weighted and constrained consensus control method was introduced to achieve platoon formation and robustness against disturbances, vehicle additions and departures, as well as communication channel uncertainties. Convergence rates were used as a performance measure to evaluate additional benefits of different communication topologies in improving platoon formation, robustness, and safety.

Communication channels insert new dynamics into control loops and influence closed-loop system performance. Impact

of communications on networked control systems can be treated by viewing communication systems as added uncertainties and constraints [9], [10], [11], [12], [13]. In [14], an in-depth study of coordinated control and communication design was conducted in which TCP-based communication protocols were employed. The main consequence of the TCP channel uncertainties is signal transmission delays. The detrimental effects of random delays on vehicle safety were investigated and coordinated control/communication design was investigated.

This paper continues our work in [14] but concentrates on block erasure channels [15]. Majority of inter-vehicle wireless communications use either a directional media such as infrared signals or broadcast radio waves including VHF, micro, and millimeter waves. The mainstream of media access control is wireless LAN and 3G distributed access, whose data flows are subject to packet losses. Analytical models of reliability of the IEEE 802.11p in VANETs safety [16] and performance evaluations of safety in Dedicated Short Range Communications (DSRC) have been studied in [17]. Erasure rate, packet loss or packet delivery rate eventually comes to creating a randomly switching networked system that impacts control performance significantly. By comparing different information structures which utilize radar distance sensors and wireless communication channels, we characterize some intrinsic relationships between communication resources and control performance. The findings of this paper provide useful guidelines on communication resource allocations and vehicle coordinations in vehicle safety systems.

The main contributions of this paper are in the following aspects. (1) This paper establishes quantitatively the impact of erasure channels on vehicle safety in a platoon framework. This is achieved by first relating erasures to randomly switching network topologies. Then, impact on safety of such networked control systems is established. (2) Relationships among channel throughput, safety, and highway utility are derived. Such relationships can be used to guide integrated design of control and communications. (3) Platoon communication design involves information content selection, network topology choice, and resource allocation. We establish results relating platoon safety to information contents (such as vehicle distance, speed, braking action), network information topologies, and bandwidth allocations.

The rest of the paper is organized as follows. Section II introduces the basic platoon control problem, safety issues, and control strategies. Section III details typical communication scenarios. Communication channel erasure characterization and related packet delivery rates (PDR) are presented. Under

Lijian Xu and Le Yi Wang are with the Department of Electrical and Computer Engineering, Wayne State University, Detroit, Michigan 48202. Email: dy0747@wayne.edu (Xu), lywang@wayne.edu (Wang)

George Yin is with the Department of Mathematics, Wayne State University, Detroit, MI 48202. Email: gyin@math.wayne.edu

Hongwei Zhang is with the Department of Computer Science, Wayne State University, Detroit, MI 48202. Email: hongwei@wayne.edu

This research was supported in part by the National Science Foundation under grant CNS-1136007.

some simplified schemes, basic relations are derived, including speed-distance relationship for safe stopping distance and collision avoidance, distance progression in a platoon, and PDR-distance functions. Section IV investigates the impact of information structure and channel erasures. Typical scenarios of communication channel erasures are considered in Section V. Finally, Section VI discusses implications of the results of this paper and points out some potential extensions.

II. REVIEW ON VEHICLE DYNAMICS AND PLATOON INFORMATION STRUCTURE

This section briefly reviews the system formulation for studying vehicle safety issues which was introduced and detailed in [14]. We are concerned with the coordination of vehicles in a highway platoon. The following simplified yet representative vehicle dynamic models from [32] are used as a benchmark case for our exploration

$$m\dot{v} + f(v) = F, \quad (1)$$

where m (Kg) is the consolidated vehicle mass (including the vehicle, passengers, etc.), v is the vehicle speed (m/s), $f(v)$ is a positive nonlinear function of v representing resistance force from aerodynamic drag and tire/road rolling frictions, and F (Newton or Kg-m/s²) is the net driving force (if $F > 0$) or braking force (if $F < 0$) on the vehicle's gravitational center. Typically, $f(v)$ takes a generic form $f(v) = a + bv^2$, where the coefficient $a > 0$ is the tire/road rolling resistance, and $b > 0$ is the aerodynamic drag coefficient. These parameters depend on many factors such as the vehicle weight, exterior profile, tire types and aging, road conditions, wind strength and directions. Consequently, they are usually determined experimentally and approximately. This paper is focused on longitude vehicle movements within a straight-line lane. Consequently, the vehicle movement is simplified into a one-dimensional system.

Vehicles receive neighborhood information by using sensors and communication systems. We assume that radar distance sensors are either installed at the front or rear of the vehicle. The sensor information will be limited to distances. In contrast, a communication channel from vehicle i to vehicle j can transmit any information that vehicle i possesses such as distance, speed, pedal action (braking). For concreteness, we will use a basic three-car platoon to present our key results. Although this is a highly simplified platoon, the main issues are revealed clearly in this system. Three information structures are studied, shown in Fig. 1. Information Structure (a) employs only front sensors, implying that vehicle 1 follows vehicle 0 by measuring its front distance d_1 , and then vehicle 2 follows vehicle 1 by measuring its front distance d_2 . For safety consideration, this structure provides a benchmark for comparison with other information structures. Information Structure (b) provides both front and rear distances. Then Information Structure (c) expands with wireless communication networks.

The platoon in Fig. 1 has the following local dynamics.

$$\begin{cases} \dot{v}_0 = \frac{1}{m_0}(F_0 - (a_0 + b_0v_0^2)) \\ \dot{v}_1 = \frac{1}{m_1}(F_1 - (a_1 + b_1v_1^2)) \\ \dot{v}_2 = \frac{1}{m_2}(F_2 - (a_2 + b_2v_2^2)) \\ \dot{d}_1 = v_0 - v_1 \\ \dot{d}_2 = v_1 - v_2, \end{cases} \quad (2)$$

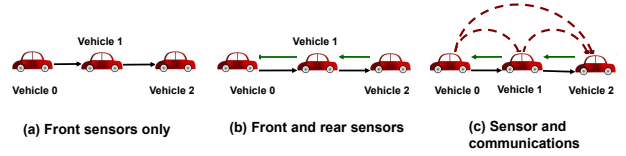


Fig. 1. Three main information structures: (a) Only front distance information is available for vehicle control. (b) Both front and rear distances are available. (c) Additional information is transmitted between vehicles.

where F_0 is the leading vehicle's driving action and viewed as an external disturbance, and F_1 and F_2 are local control variables. For safety consideration, the inter-vehicle distances d_1 and d_2 must maintain a minimum distance $d_{min} > 0$. To ensure that vehicles 1 and 2 have a sufficient distance to stop when the leading vehicle 0 brakes, a normal distance d_{ref} is imposed. There are numerous control laws which have been proposed or commercially implemented [18], [19]. To study impact of communication uncertainty on platoon safety, we will use certain simple and fixed control laws. The control law is shown in Fig. 2. We denote this function as $F = g_1(d)$. Similarly, if vehicle i 's speed information is transmitted to another vehicle j , the receiving vehicle uses a control strategy generically represented by a function $F = g_2(v_j - v_i)$, depicted in Fig. 3.

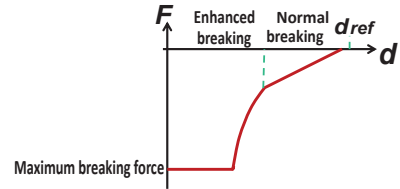


Fig. 2. Braking functions based on distance information

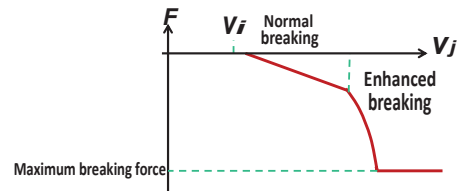


Fig. 3. Braking functions based on speed information

III. INFORMATION STRUCTURES AND COMMUNICATION MODELS

Inter-vehicle distances are most commonly measured by radars. Radar sensors provide a stream of measurement data, typically using 24, 35, 76.5, and 79 GHz radars. In general, radar sensor measurements are influenced by many factors that limit their accuracy and reliability. These include signal attenuation by the medium, beam dispersion, noises, interference, multi-object echo (clutter), jamming, etc.; see [20] for further detail. On the other hand, when communication channels

are employed, channel uncertainties become essential features in control design consideration. This paper concentrates on communication uncertainties from erasure channels, which are described next.

A. Erasure Channels in Wireless Communications

The block-erasure channel represents a channel model where transmitted packets are either received or lost. The loss of a packet may be caused by erasure of one or multiple bits within the packet during transmission. Typically, block-erasure channels are simple models for fading channels. Due to power limitation, transmission noises, signal interferences, some codewords in a packet may be completely lost [21], [22], [24]. Probability of packet erasures can be reduced by introducing error detection and correction bits, which increase data lengths and reduce information flow rates.

We consider block-erasure channels with certain channel codings that include error detection. Generic discussions are sufficient at this point, and the actual channel coding schemes will be specified in case studies in Section V. In this protocol, channel error detecting codes such as parity-check matrices are encapsulated and are used by the receiver to either detect transmission errors or in some cases correct the missing or erroneous bits. The detection/correction mechanism is shown in Fig. 4.

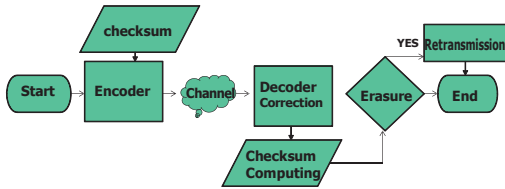


Fig. 4. An erasure channel with check-sum error detection and re-transmission

During one round-trip of this scheme starting at time t_k , the source generates a data block, which is channel coded with codeword c_{t_k} and transmitted. Due to channel uncertainties, the decoder receives the codeword \hat{c}_{t_k} with possible erasure of one or more bits. After decoding and error correcting, the receiver either acknowledges receipt of the data, or indicates a packet erasure. Suppose that the round-trip time for this scheme is τ . If $t_k + \tau < t_{k+1}$, a re-transmission is implemented and the above transmission process renews.

At t_{k+1} , the data is either received correctly or declared to be lost. In the later case, the channel is equivalently disconnected during $[t_k, t_{k+1})$ since no data are received. Since this event is random, the channel is modelled as a random link, with probability p_k to be linked and $1 - p_k$ to be disconnected. Applying this scenario to all channels, we have a randomly switching network topology such that the probability for each topology is generated from individual link connection probabilities.

In the next subsections, we derive probabilistic models for erasure channels. Our pursuit involves two objectives: (1) Understand what is the minimum signal-to-noise ratio (SNR) for a required safety level. To this end, we must derive erasure

probability's lower bounds. Information-theoretical analysis will be employed. (2) Employ a practical system and its corresponding erasure probability characterization to characterize concretely the required information for platoon control. In a VANET framework, inter-vehicle communications can use either convolution code or block code. Conventionally, convolution codes are still the first choice for applications which require low data-structure delays. Low density parity-check (LDPC) is always chosen if one focuses on low SNR. Theoretically, when the block code size $n \rightarrow \infty$, bit error rate (BER) $\rightarrow 0$. Obviously, the longer the block length is, the larger the delay time is resulted, due to computing time complexity. This issue has been largely resolved with implementation of LDPC convolutional codes [23] with higher performance hardware and software during the past 10 years. We use LDPC coding as a benchmark coding scheme to carry out our study. The LDPC codes have appealing properties in their theoretical foundation and implementation efficiency. Their main advantages in computational efficiency and code length utility have resulted in many successful commercial products.

B. Probabilistic Error Models of Erasure Channels

We consider an erasure channel whose packet contains B bits for information transfer.¹ The information bits are divided and used either for data or for error checks. In this section, it is not necessary to specify such divisions. For simplicity, all coding schemes in this paper are over the binary field $\mathbb{F}_2 = \{0, 1\}$, although the results of this paper can be easily extended to other fields. For the same reason, we consider standard erasure channels instead of block-erasure channels, although it is straightforward, but a little tedious in expressions, to derive probabilistic error models for block-erasure channels.

To transmit a code S of size $K = \log_2 |S|$ with the codeword of length L , we have the coding rate $r = K/L$ per channel usage. Let the codeword be denoted by $c = [c_1, \dots, c_L]$ where $c_j \in \{0, 1\}$ is the j th bit of the codeword c . The erasure pattern is indicated by the vector $\eta = [\eta_1, \dots, \eta_L]$ such that $\eta_j = 1$ means that the j th bit is erased, and $\eta_j = 0$ indicates the j th bit is received correctly.

We consider a two-time-scale scenario for link communication and control. Control actions are updated every T seconds, and the communication round-trip time is τ . For simplicity, assume $T = k\tau$ for some integer $k \geq 1$. If a transmission results in an ambiguity at the receiver's side such that the transmitted code cannot be uniquely determined, it will label it as "failure" for this transmission and a re-transmission request is returned to the sender. Consequently, the maximum number of transmissions of the same code during T is k . It should be pointed out that when ambiguity arises, we do not use any method to break the tie which will cause a possible erroneous decoding, but rather demand a re-transmission. As a result, we either receive the correct code or do not have information at all.

¹As a common practice for information and error analysis, packet heading and other auxiliary segments are not considered in our analysis.

Let the minimum Hamming distance of S be $d \geq 1$.² It follows that if a transmission causes less than $d - 1$ erasures, the transmitted code can be uniquely detected. For a unified treatment and in consideration of the worst-case scenario, we consider erasures with d erasures or more as a failed transmission in our probabilistic models for error analysis.³ For related but different error models and channel coding methods in erasure channels, we refer the reader to [15], [21], [22], [24] for further details.

Suppose that bit transmissions are independent and identically distributed (i.i.d.) and the bit erasure probability is ε . In one transmission, the error probability can be calculated from the standard Bernoulli trials and binomial distributions [29],

$$\begin{aligned} P_e^1 &= \mathbf{P}\{\eta : \eta \text{ contains 1's at } d \text{ locations or more}\} \\ &= \sum_{j=d}^L \mathbf{P}\{\eta : \eta \text{ contains 1's at exactly } j \text{ locations}\} \\ &= \sum_{j=d}^L \binom{L}{j} \varepsilon^j (1-\varepsilon)^{L-j} \\ &= \sum_{j=d}^L \frac{L!}{j!(L-j)!} \varepsilon^j (1-\varepsilon)^{L-j}. \end{aligned}$$

Under independent transmissions of channel usage, we have the link erasure probability after k usages of the channel as

$$P_e^k = (P_e^1)^k = \left(\sum_{j=d}^L \frac{L!}{j!(L-j)!} \varepsilon^j (1-\varepsilon)^{L-j} \right)^k. \quad (3)$$

It is noted that in the worst-case sense, the probability model in (3) is exact. For practical codes, (3) provides an upper bound on the erasure errors during one time interval of control action update.

Example 1: Suppose that the code length is $L = 20$ and the minimum Hamming distance is d . Fig. 5 depicts packet erasure probabilities as functions of bit erasure probabilities ε under various minimum Hamming distances d . Furthermore, when communication round-trip time τ is smaller than control updating time T , multiple re-transmission becomes possible and can be used to reduce packet erasure probabilities. This is shown in Fig. 6 under a code of length $L = 20$ and minimum Hamming distance $d = 4$.

C. Communication Resources and Erasure Probabilities

The bit erasure probability ε depends on communication resources such as power and bandwidths, and also transmission media. In a mobile system such as highway vehicles, vehicle-to-vehicle (V2V) communication links are affected by inter-vehicle distances, weather conditions, obstacles, interference, signal fading, etc. Consequently, a detailed and accurate description of bit erasure probability for a practical system is ad hoc and extremely difficult. On the other hand, the principles

²The Hamming distance between two codes is the number of positions at which the corresponding symbols are different.

³Depending on the actual code, some specific erasure patterns with d or more bit erasures may not result in ambiguity. However, such cases defy unified treatment. For practical implementations, these details can be considered to improve transmission efficiency.

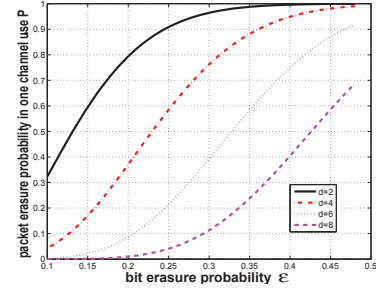


Fig. 5. Packet erasure probabilities under one transmission: $L = 20$

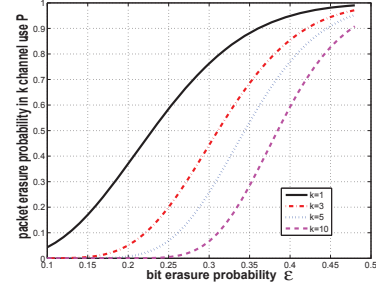


Fig. 6. Packet erasure probabilities under k transmissions: $L = 20$, $d = 4$

and generic function forms of bit erasure probability can be established and used as a guideline in design considerations. This subsection discusses such principles and function forms.

We use the Binary Additive White-Gaussian-Noise Channel (BAWGN) for this exploration. The source symbol x takes values in $\{-1, 1\}$. With the BPSK (Binary Phase-Shift Keying), signal energy E_N , additive channel noise of independent zero-mean Gaussian distribution with variance σ^2 , and hard-decision decoding, it is well known [31, Chapter 4] that the error probability (including both events “1 is sent but 0 is received” and “0 is sent but 1 is received”) is

$$\varepsilon = Q(\sqrt{E_N/\sigma^2}), \quad (4)$$

where the Q function is

$$Q(x) = \int_x^\infty \frac{1}{\sqrt{2\pi}} e^{-\frac{y^2}{2}} dy.$$

In our framework, this error is interpreted as the erasure probability with the understanding that erasure detection is achieved by channel coding and error detection decoding.

Here ε is a function of the E_N/σ^2 . Also, following the standard practice of representing noise variance by its power $N_0 = 2\sigma^2$ (single-sided power-spectral density), we have

$$\varepsilon = Q(\sqrt{2E_N/N_0}). \quad (5)$$

In this paper, we use E_N/N_0 as a representation of the SNR, although different notions of SNR exist. Combining (3) and (5), we may link the packet erasure probability directly to the SNR

$$P_e^k(E_N/N_0) = \left(\sum_{j=d}^L \frac{L!}{j!(L-j)!} (Q(\sqrt{2E_N/N_0}))^j (1 - Q(\sqrt{2E_N/N_0}))^{L-j} \right)^k. \quad (6)$$

Usually, the SNR is expressed in dB, namely $10 \log_{10}(E_N/N_0)$. Fig. 7 illustrates how the SNR of the channel affects the packet erasure probability.

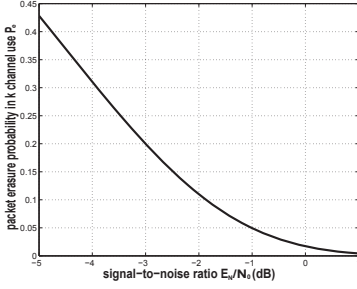


Fig. 7. Packet erasure probabilities as a function of the signal-to-noise ratio

IV. IMPACT OF INFORMATION STRUCTURES AND CHANNEL ERASURE

This section lays the foundation for performance analysis in a vehicle safety framework. We concentrate on impact of erasure channels.

A. Evaluation Scenarios

To investigate impact of information structures and contents on platoon safety, we use the following basic scenarios in which only key elements are represented; see [14].

Typical vehicle data from [32] are used: Under the MKS (metre, kilogram, second) system of units, the vehicle mass m has the range 1400 – 1800 Kg; and the aerodynamic drag coefficient b has the range 0.35 – 0.6 Kg/m. During braking, a (as the rolling resistance) is changed to tire/road slipping, which is translated into the braking force F (negative value in Newton).

Three identical cars form a platoon, as shown in Fig. 1. The vehicle masses are $m_0 = m_1 = m_2 = m = 1500$ Kg. The tire/road rolling coefficient $a = 0.01$ and the aerodynamic drag coefficients $b_0 = b_1 = b_2 = 0.43$. The nominal inter-vehicle distance $d_{ref} = 40$ m. The cruising platoon speed is 25 m/s (about 56 mph). The road condition is dry and the maximum braking force is 10000 N. This implies that when the maximum braking is applied (100% slip), the vehicle will come to a complete stop in 3.75 second. The braking resistance can be controlled by applying controllable forces on the brake pads.

The braking function is

$$F = g_1(d) = \max\{k_1(d - d_{ref}) + k_2(d - d_{ref})^3, -F_{max}\} \quad (7)$$

where $d_{ref} = 40$ (m), $k_1 = 50$, $k_2 = 4$, $F_{max} = 10000$ (N). The function applies smaller braking force when the distance is only slightly below the reference value, but increases the braking force more dramatically in a nonlinear function when the distance reduces further until it reaches the maximum braking force.

The basic information structure is to use front sensors only. For the three-car platoon in Fig. 1 and the control law $F =$

$g_1(d)$ in (7), the closed-loop system becomes

$$\begin{cases} \dot{v}_0 = \frac{1}{m_0}(F_0 - (a_0 w_0 + b_0 v_0^2)) \\ \dot{v}_1 = \frac{1}{m_1}(g_1(d_1) - (a_1 w_1 + b_1 v_1^2)) \\ \dot{v}_2 = \frac{1}{m_2}(g_1(d_2) - (a_2 w_2 + b_2 v_2^2)) \\ \dot{d}_1 = v_0 - v_1 \\ \dot{d}_2 = v_1 - v_2 \end{cases} \quad (8)$$

Fast Braking Scenario: Suppose that the leading vehicle uses a braking force 5000 N, which brings it to a stop from 25 m/s in 7.5 second. The distance trajectories of d_1 and d_2 are shown in the right plots of Fig. 8. In this case, the minimum distances are 20.6 m for d_1 that is acceptable, but 0 m for d_2 . This means that vehicle 2 will collide with vehicle 1 during the transient time. For comparison, the left plots show that under slow braking (a much smaller braking force by the leading vehicle), the platoon safety is not an issue under the current control strategy. We will use this fast braking scenario to understand benefits of communications in the following subsections.

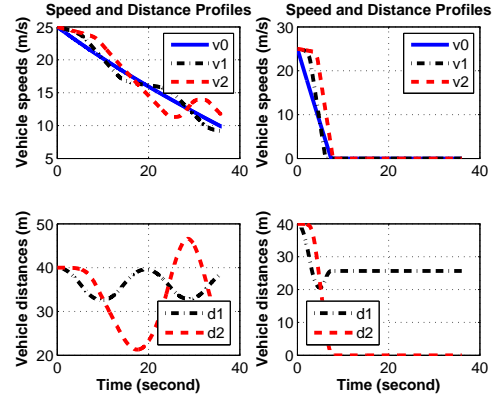


Fig. 8. Distance trajectories under slow and fast braking.

B. Information by Communications and Channel Erasure

We next expand on the information structure by adding new information via communications. Communications introduce a variety of uncertainties, such as latency, jitter, and packet loss. We only focus on the effect of packet loss.

Example 2: We first consider distance-independent package erasure rates. Under the above evaluation scenario, now vehicle 1 sends d_1 information to vehicle 2 by communication. As a result, vehicle 2 can use both d_1 and d_2 in its control function; see Fig. 9.

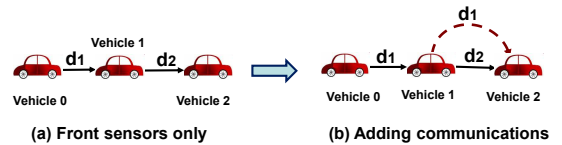


Fig. 9. Enhanced information structure by sending d_1 to vehicle 2 by communication links in Example 2

Suppose that vehicle 2 modifies its braking control function from the previous $F_2 = g_1(d_2)$ to the weighted sum $F_2 =$

$0.5g_1(d_2) + 0.5g_1(d_1)$ that uses both distances. Assuming that the communication channels are secure (no erasures or $P_e^k = P_e = 0$), the resulting speed and distance trajectories are displayed in the left plots of Fig. 10. With information feeding of d_1 into vehicle 2, vehicle 2 can slow down when d_1 reduces before d_2 changes. Consequently, the minimum distances are increased to 20.6 m for d_1 and to 15.9 m for d_2 , both are within the safety region.

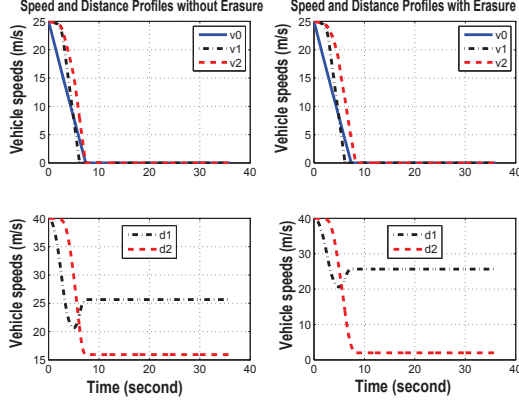


Fig. 10. Distance trajectories when the distance information d_1 is made available to vehicle 2 and with Erasure rate 0 and 0.4.

Channel erasure has significant impact on vehicle safety. To show this, assume that the packet erasure probability is increased to $P_e = 0.4$. The right plots of Fig. 10 highlight a drastic reduction of the minimum distances to near zero. Fig. 11 illustrates the dependence of the minimum distances on the link erasure probability.

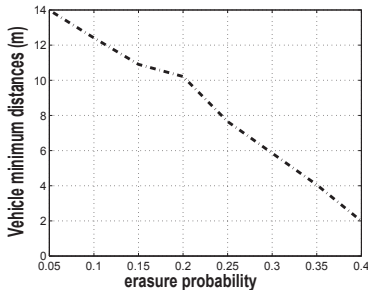


Fig. 11. Minimum inter-vehicle distances and erasure probabilities on distance information

Example 3: We now add the speed information of the leading vehicle to both vehicles 1 and 2 by communication. For the same three-car platoon under the same initial conditions as Example 2, we add the leading vehicle's speed v_0 into the information structure. This information is transmitted (or broadcasted) to both vehicles 1 and 2. Under the **Fast Braking** scenario as in Example 2, suppose that vehicles 1 and 2 receive the additional speed information v_0 , resulting in a new information structure.

From the control functions of Example 2, additional control actions $g_2(v_0 - v_1)$ and $g_2(v_0 - v_2)$ are inserted. The resulting speed and distance trajectories are displayed in the left plots of Fig. 12. Now, the minimum distances are increased to

28.3 m for d_1 and 27.1 m for d_2 , a much improved safety performance.

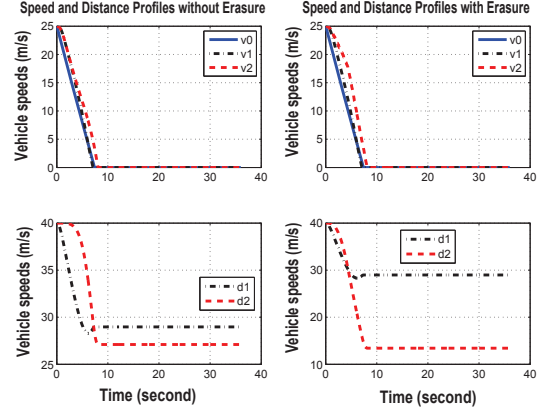


Fig. 12. Distance trajectories when both distance and speed information transmitted with erasure rate 0 and 0.5.

Example 4: Similarly, we can consider impact of erasure channels for v_0 and d_1 information as in Example 2. Under the same system and operating condition as Example 3, we assume that the communication channel for the speed v_0 and d_1 information is an erasure channel. The left plots of Fig. 12 represent the secured channel without erasure. If the packet erasure probability is increased to $P_e = 0.5$, the right plots of Fig. 12 highlight a reduction of the minimum distance to 13.89 (m), which is less than an acceptable minimum distance d_{min} . Fig. 13 depicts the dependence of the minimum distances on the link erasure probability on transmission of d_1 and v_0 information.

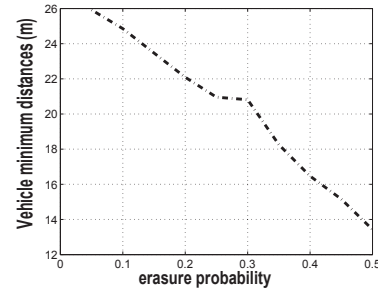


Fig. 13. Minimum inter-vehicle distances and erasure probabilities on speed and distance information

Intuitively, if the leading vehicle's braking action can also be communicated, the following vehicles can act much earlier than their measurement data on vehicle movements. To evaluate benefits of sending the driver's action, we add the braking event information of the leading vehicle to vehicle 2 by communications.

Example 5: For the same three-car platoon under the same initial conditions as Example 3, we add the leading vehicle's braking event information F_0 into the information structure. From the control functions of Example 3, an alternative control action F_0 is inserted when $d_2 < d_{ref} = 40$ m. The resulting speed and distance trajectories are displayed in the left plots of Fig. 14. Now, the minimum distances are increased to 28.3m

for d_1 and 30.6m for d_2 , a much improved safety over the case in Example 3.

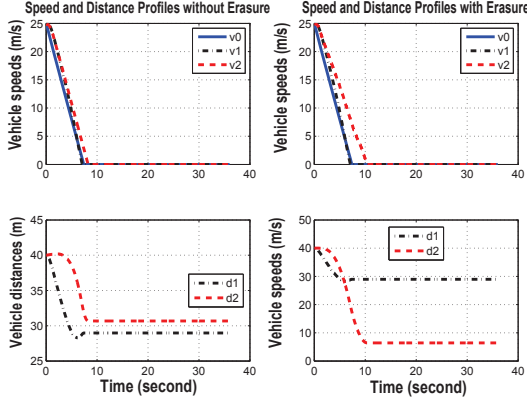


Fig. 14. Distance trajectories with added braking event information.

Example 6: Under the same system and operating condition as Example 5, we assume that the communication channel for F_0 , v_0 , and d_1 is an erasure channel with erasure probability $P_e = 0.25$. The right plots of Fig. 14 demonstrate a drastic reduction of the minimum distance to 7.07 (m), it is less than an acceptable minimum distance d_{min} .

Fig. 15 summarizes the dependence of the minimum distance on the link erasure probability on transmission of d_1 , v_0 , and F_0 . It shows that brake event is more sensitive to the erasure probability than the distance and speed information.

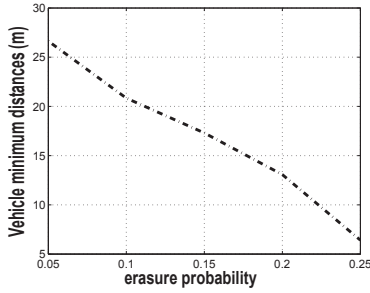


Fig. 15. Minimum inter-vehicle distances and erasure probabilities

V. CASE STUDIES

This section presents several cases that include more details on communication systems. Due to the complexity of traffic conditions, environments, and communication facility heterogeneity, our case studies consider several basic features and main communication resources.

A. Package Erasure Rate Implications of Inter-vehicle Distance

1) *Distance-Dependent Signal Attenuation:* There are many factors at the physical level that affect a link's package erasure rates. Here, we consider the main factor from signal fading due to variations in inter-vehicle distances.

Suppose that the leading vehicle broadcasts a complex sinusoid $e^{2\pi i f t}$. The signal strength at the receiving site of distance d behind the leading vehicle is typically modeled as

$$E_s = \frac{\alpha_s(\theta, \psi, f) e^{2\pi i f (t-d/c)}}{d} \quad (9)$$

where (θ, ψ, f) are the vertical angle, horizontal angle, and carrier frequency, respectively, and c is the speed of light. What is relevant here is the fact that the power radiated per unit area attenuates with rate $1/d^2(t)$. This in turn implies a decaying SNR as the distance increases. Consequently, P_e^k in (6) becomes a function of the inter-vehicle distance.

Also, communication uncertainties, such as signal reflections, inter-symbol interferences, and Doppler shift, will further increase the error probability ε . To accommodate more realistic vehicle communication environments, in our case studies we employ the experimental package delivery rate (PDR) data from [33], shown in Fig. 16. Here, the relationship of PDR and P_e is $\rho = 1 - P_e$. For example, in a typical rural road environment, the PDR decreases from $\rho \approx 0.936$ in the range of 0 – 50 m to $\rho \approx 0.391$ in the range of 450 – 500 m.

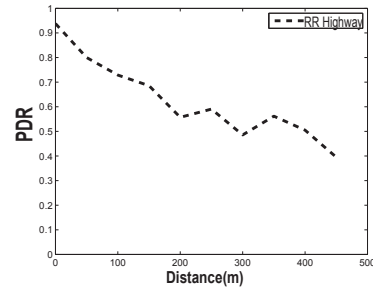


Fig. 16. The impact of separation distance (with the 95% confidence interval). In this figure, a bin of 20 packets is used to calculate PDR values.

2) *Dedicated Short Range Communications:* The PDR of a link depends also on communication protocols. Currently, the most commonly accepted vehicle communication protocol is IEEE 802.11p, which supports DSRC. IEEE 802.11p is a modified version of IEEE 802.11(WIFI) standard. DSRC is a short-to-medium range communications service that supports both public and private operations in roadside-to-vehicle and vehicle-to-vehicle communications environments. It is one of the most effective means to deliver rapidly real-time data. In the US, a spectrum of 75 MHz from 5.850 GHz to 5.925 GHz is allocated for DSRC applications. Within the spectrum, 5 MHz is reserved as the guard band, and seven 10-MHz channels are configured into one control channel (CCH) and six service channels (SCHs). The CCH is reserved for carrying high-priority short messages or management data, while other data are transmitted on the SCHs.

There are many experimental studies of IEEE 802.11p on freeway environments. Since we are only concerned with PDR, we quote here the studies in [33] which contains extensive experimental results of PDR from many possible contributing factors, such as inter-vehicle distance, signal propagation environment, relative velocity, effective velocity, received signal strength, and transmission power and modulation rate.

B. Probabilistic Characterization of PDR and Sampling Time on Vehicle Safety

Impact of the PDR on vehicle safety can be analyzed by a simplified transmission model. In this model, when a packet is lost the measured variable is not delivered. As a result, the controller must use the previous value in its control actions. Mathematically, this is similar to a sampling process with random sampling times.

Suppose that the baseline sampling interval is τ_0 . At $k\tau_0$, we use a link-connection variable γ_k to indicate if the packet is delivered ($\gamma_k = 1$) or lost ($\gamma_k = 0$). As a result, assuming that γ_k is independent and identically distributed (i.i.d.), we denote the PDR by $\rho = P\{\gamma_k = 1\}$. Fig. 17 shows a sample path under $\rho = 30\%$ and $\tau_0 = 0.2$.

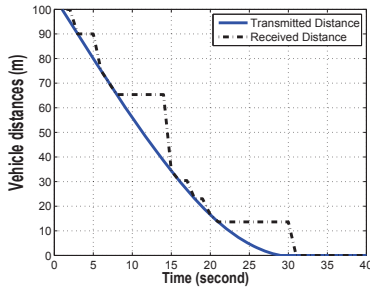


Fig. 17. Transmitted d_k and received \tilde{d}_k

To give a sense on how the PDR will influence the vehicle safety, we consider a simplified two-vehicle model, with vehicles V_0 and V_1 shown in Fig. 18. In this model, the actual inter-vehicle distance is d but the vehicle controller on V_1 can only use the received \tilde{d} , rather than the actual distance d , to control its braking action.

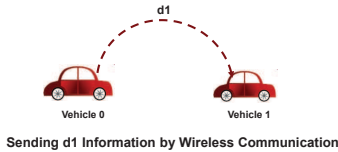


Fig. 18. Two-vehicles model with wireless communication only

The vehicle velocities are v_0 and v_1 , respectively. Define $v = v_1 - v_0$. Then the two-car system dynamics is

$$\begin{cases} \dot{v} &= -\frac{f(\tilde{d})}{m_0} \\ \dot{\tilde{d}} &= -v. \end{cases} \quad (10)$$

The received distance information under sampling interval τ_0 can be represented by

$$\tilde{d}_k = \begin{cases} d_k, & \text{if } \gamma_k = 1 \\ \tilde{d}_{k-1}, & \text{if } \gamma_k = 0. \end{cases} \quad (11)$$

Example 7: Without loss of generality, assume $v_0 = 0$. Then $v = v_1$. Vehicle masses $m_0 = m_1 = 1500$. The initial speed $v(0) = 25$ m/s and the nominal inter-vehicle distance $d_{ref} = 80$ m. The simplified feedback control function is

$$g_1(\tilde{d}) = \max\{k_1(\tilde{d} - d_{ref}), -F_{max}\} \quad (12)$$

where $k_1 = 115$, $F_{max} = 10000$ (N). Suppose that the communication channel PDR is $\rho = 70\%$ and sampling time $\tau_0 = 0.2$ second. The plot of Fig. 19 is the probabilistic distribution of the final inter-vehicle distances under 1000 repeated runs. The sample average of the final distance is $E(d_{final}) = 3.6603$ (m) and variance $\sigma^2 = 1.0757$.

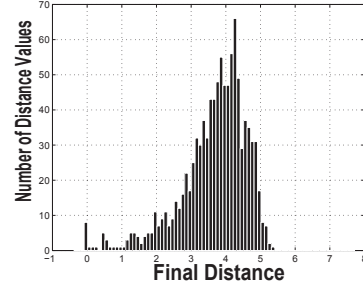


Fig. 19. Final distance distribution with repeating 1000 times

Example 8: Under the same configuration of Example 7, we now consider time-varying PDR value $\rho(t)$ that is a function of the distance. In this two-vehicle model, the impact of inter-vehicle distance on the whole trajectory of $\rho(t)$ in both open field and rural road environments is considered. The simulation results in Fig. 20 show the average final distance as a function of the initial PDR $\rho(t_0)$ varying from 0 to 1.

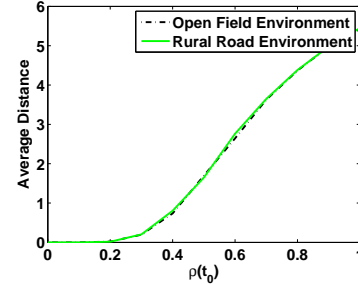


Fig. 20. Average final distance vs. distance-dependent PDR $\rho(t_0)$

Fig. 20 indicates a monotone relationship between $\rho(t_0)$ and final distance d_{final} : The higher the initial PDR $\rho(t_0)$, the earlier vehicle 1 stops. On the other hand, if we choose a shorter sampling interval $\tau'_0 < \tau_0$, namely using a faster sampling system, then more re-transmission is allowed with a given control updating interval, leading to a higher probability of data receipt. To show this, we fix PDR to $\rho = 30\%$. The simulation results in Fig. 21 demonstrate the average final distance as a function of sample time τ_0 . It shows a monotone relationship: the shorter the base sampling interval, the earlier the vehicle stops.

C. Impact of Transmission Power and Modulation Rate

We perform two case studies in this subsection with two commonly used transmission parameters: transmission power and data modulation rate. Vehicular ad hoc network (VANET) designers can control these parameters to meet platoon safety requirements. The coverage distance by a single radio link,

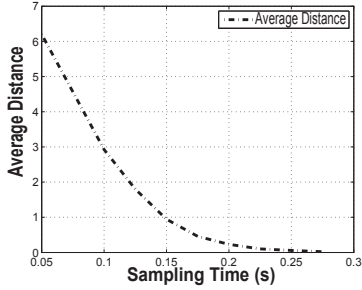


Fig. 21. Average final distance vs. varying sampling time

which ranges from 10 m to 1 km in IEEE 802.11p, depends on the transmission power, channel environment, modulation and coding schemes.

Example 9: We first exam the impact of transmission power. Wireless devices are assumed to have maximum transmission power from 0 dBm to 28.8 dBm. Fig. 22 from [33] is an experimental result relating the PDR to transmission distances. The figure describes how the PDR varies with the inter-vehicle distance under different transmission power levels while keeping other factors fixed. The transmission power varies from 10 dBm to 20 dBm in a rural road environment. It shows that higher transmission power generates higher PDRs. For example, under the same system and operating condition as Example 3, by applying the PDR curve with 20 dBm transmission power, the left plots of Fig. 23 implies that the minimum distance is 14.92 (m).

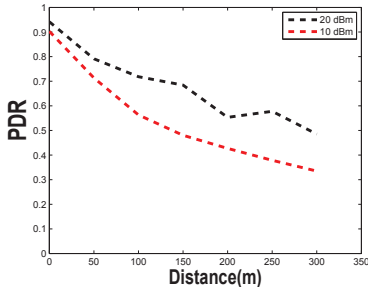


Fig. 22. PDR vs. distance under different transmission power settings in the rural road (RR) environment (with 95% confidence interval). Here, the transmission power is 10 dBm and 20 dBm. The data rate is 6 Mbps.

When the transmission power is reduced to 10 dBm, the right plots of Fig. 23 give a minimum distance 6.88 (m). It is no longer an acceptable distance.

Example 10: We now exam the impact of modulation rate. A typical curve from [33] is re-generated in Fig. 24. The figure describes how the PDR varies with the distance under different modulation rates. By applying the first PDR under modulation rate 6 Mbps, the simulation in Fig. 25 shows that the minimum distance is 12.44 (m).

On the other hand, if the modulation rate is increased to 18 Pbps, Fig. 25 shows that the minimum distance is reduced to 0 (m) and a collision occurs.

In DSRC, devices participating in V2V safety will normally be in class C with a communication zone of 400 meters and

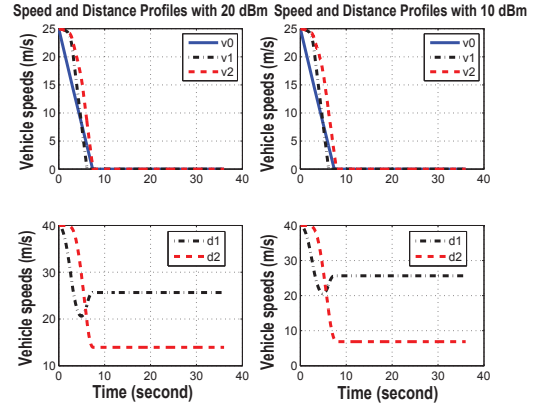


Fig. 23. Distance and speed trajectories with the leading vehicle speed information under different transmission powers.

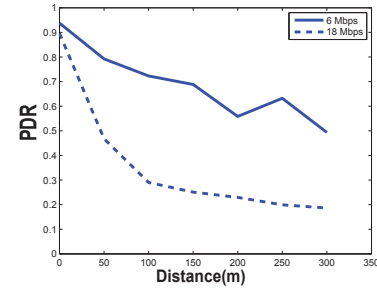


Fig. 24. PDR vs. distance under different modulation rates

maximum output power of 20 dBm [34]. Assuming a typical inter-vehicle distance of 40 meters, vehicles can access the information of 10th vehicle ahead directly. On the other hand, if we implement class D devices with a communication zone of 1 km, this radio range can cover a platoon with 25 vehicles. In safety related applications, reliable vehicle communication of information from neighbors within 10 vehicles ahead is important. If out-of-range V2V information access is necessary, it can be fulfilled by multi-hop protocols, with longer delay time.

Although we employ a three-car platoon for simplicity, it forms a generic base for studying platoon safety issues for more general platoons.

D. Improvement of Communication Performance

Platoon safety requirements as studied in the previous sections lead to required bounds on channel erasure rates. In turn, the relationship among erasure probability, sampling interval, and PDR, eventually leads to the required digital communication data rate R_i (Mbps) for the i th link in a given network topology, during a given control updating step.

In a platoon with a communication topology that contains N links, suppose that the intrinsic relationship between the communication data rate and platoon safety distance concludes that the required data rates for the links during the control updating interval $[kT, (k+1)T)$ are given by

$$R(k) = [R_1(k), R_2(k), \dots, R_N(k)]'$$

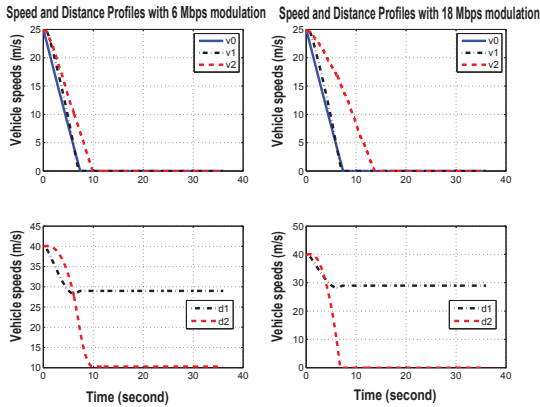


Fig. 25. Distance and speed trajectories with braking information under modulation rate of 6 Mbps and 18 Mbps.

which must be implemented by the communication system. This implies that for link i , the data of size $m_i(k) = R_i(k) \times T$ (Mb) must be transmitted.

To be concrete, we use time division multiple access (TDMA) as the communication protocol. The TDMA has been studied as a potential and promising candidate for inter-vehicle communications. Under the TDMA, the links take turns to transmit packages. The transmission time slot (and typically, one packet of data is transmitted within one time slot) is a constant time interval t^0 , which includes necessary guard times for modem preambles and Tx-Rx switch-over latencies.

Suppose that the net data size of each slot is m^0 (Mb). Then, link i will use at least $m_i(k)/m^0$ time slots to complete its data transmission. The actual communication resource consumptions depend on communication scheduling strategies. We use total time slots as the resource consumption to compare different resource allocation schemes and seek the optimal scheduling.

In each data frame of the TDMA, every link can have a maximum of one time slot. For the N link topology, each TDMA frame has a maximum of N slots. For a TDMA frame of duration T_{fr} , the frame size is defined as the number of slots it contains: $fr = T_{fr}/t^0$. Under a uniform frame structure, each frame contains the fixed number of N slots and each link is assigned one slot in every frame, regardless if it uses it or not. This strategy is simple, but wastes a lot of resources. Indeed, let

$$R_{max}(k) = \max\{R_1(k), R_2(k), \dots, R_N(k)\}.$$

This implies that

$$m_{max}(k) = \max\{m_1(k), m_2(k), \dots, m_N(k)\} = R_{max}(k) \times T,$$

and the number of frames in $[kT, (k+1)T)$ is $L(k) = R_{max}(k)T/m^0$. Consequently, the total number of consumed slots is $NL(k)$.

We propose a new optimal scheduling algorithm for networked communication management for platoon safety. This optimal scheduling can achieve the minimum average frame dimension for each platoon control step. Denote the j th frame size, $j = 1, \dots, L(k)$ by $fr^j(k)$. Then, the average frame size

is defined as

$$\overline{fr}(k) = \sum_{j=0}^{L(k)} fr^j(k)/L(k),$$

which is used as a performance measure for communication scheduling strategies. The optimal scheduling seeks

$$\overline{fr}_{opt}(k) = \min \overline{fr}(k)$$

under the condition that the required $R(k) = [R_1(k), R_2(k), \dots, R_N(k)]'$ is satisfied.

Our coordinated communication scheduling involves strategies that assign data frames dynamically with variable sizes to save communication resources.

Lemma 1: A time-slot scheduling mechanism at a platoon-control updating step is optimal if

$$\overline{fr}(k) = \frac{\sum_{j=1}^N R_i(k)}{R_{max}(k)} := \overline{fr}_{opt}(k). \quad (13)$$

Proof: The total number of time slots needed to complete data transmission under the required data rates $R(k) = [R_1(k), R_2(k), \dots, R_N(k)]'$ is at least $T \sum_{j=1}^N R_i(k)/m^0$. Since each frame allows to transmit at most one packet for each link, the total number $L(k)$ of frames is

$$L(k) = \frac{R_{max}(k)T}{m^0}. \quad (14)$$

Consequently, the average $\overline{fr}(k)$ is bounded below by

$$\overline{fr}(k) \geq \frac{T \sum_{j=1}^N R_i(k)/m^0}{R_{max}(k)T/m^0}.$$

As a result, any scheduling scheme that achieves the lower bound is optimal. \square

Now we propose a new scheduling scheme that achieves the optimal slot allocation.

Time-Slot Scheduling Algorithm

Data Rate Based Priority: Due to the different data rate requested by different links, we assign a higher priority for a link with higher data rate. For example, a slot is assigned to link j as long as there is no higher priority links in the same frame.

Data Rate Based Slot Allocation:

- 1) The data block of each link is divided into packets of size m^0 , queued in the link's own buffer. All the queues form a data bank for the time-slot scheduler.
- 2) Starting from frame 1, the time-slot scheduler takes one packet from each link in the order of the link's priority. The queues of the links are reduced by one.
- 3) At the j th frame, if a link's queue is empty, the time-slot scheduler removes this link from its pool.
- 4) The steps (2) and (3) are repeated until the data bank is empty.

Theorem 1: The Time-Slot Scheduling Algorithm is optimal.

Proof: We only need to show that this algorithm achieves the lower bound $\frac{T \sum_{j=1}^N R_i(k)/m^0}{R_{max}(k)T/m^0}$.

The scheduling algorithm ensures that (1) all time slots are always assigned to links whose queue are not empty; (2) any

link that has completed data transmission and has an empty queue is removed from the data bank. Consequently, by using variable frame sizes and the these two main properties, no time slot is assigned but not used. It follows that the total number of the used time slots is precisely $T \sum_{j=1}^N R_i(k)/m^0$.

On the other hand, the priority assignment ensures that the link with R_{max} will completely determine the number of frames, which will be exactly $L(k) = \frac{R_{max}(k)T}{m^0}$.

These two properties imply that the average $\bar{f}r(k)$ under this algorithm is $\frac{T \sum_{j=1}^N R_i(k)/m^0}{R_{max}(k)T/m^0}$. This completes the proof. \square

Remark 1: Some synchronization with platoon control is needed. During implementation of the above Time-Slot Scheduling Algorithm, the TDMA may need to dynamically release or borrow communication resources to maintain an average optimal resource consumption.

(1) If the control updating interval T is relatively large and reliable platoon safety requirements are not stringent, then the TDMA allocation of $L(k)$ frames can be accomplished in T , namely, communication is faster than what is required by control, the TDMA releases unused time slots to other users.

(2) If the control demands are beyond the available TDMA resource, the TDMA begins to borrow slots from other frequency bands so that more communication resources can be made available. With these additional synchronization methods, overall data rates can be successfully realized to achieve platoon control goals.

(3) With the above optimal algorithm, the usage of communication resources is reduced to

$$\eta = \frac{\sum_{i=1}^N R_i}{NR_{max}}. \quad (15)$$

Example 11: We use the three-vehicle model with the same initial conditions of Example 5. Vehicle 2 only accesses the leading vehicle's braking information. Figure 15 shows that a safety distance of $d = 15.14$ m can still be achieved even when the data rate R_2 of the link between vehicle 0 and vehicle 2 drops to $1/77$ of R_1 .

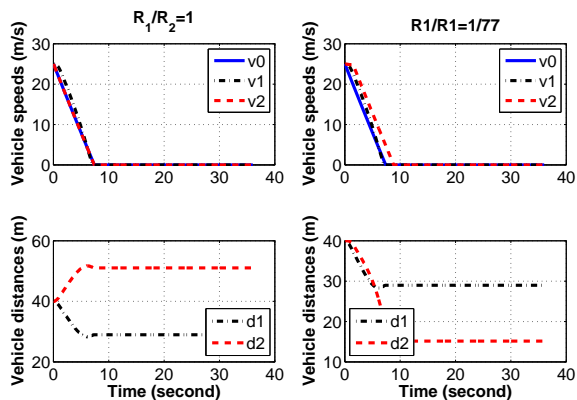


Fig. 26. Final distance vs data rates

Suppose that a typical IPv6+UDP/TCP protocol is used in such systems. Each package includes IPv6 overhead, data,

error checking bits and acknowledgement. By using the Time-Slot Scheduling Algorithm, the average frame size is reduced to request only $1.012/2 = 50.60\%$ in data size to meet the control goal of safety distance. This dramatically improves the communication bandwidth usage.

VI. DISCUSSIONS AND CONCLUDING REMARKS

This paper investigates the interaction between control and communications, in the framework of highway platoon safety. Information structure, information content, and information reliability have been taken into consideration in this study. Communication systems introduce a wide variety of uncertainties. To be concrete, we have selected communication PDRs as a key uncertainty in this study.

The main results of this paper demonstrate that communications provide critical information that can enhance vehicle safety effectively beyond distance sensors. In fact, from our simulation and analysis studies, platoon control may mandate communications for additional information. Although traditionally, distance and vehicle speed are immediate candidates for transmission, our results show that drivers' braking events contain very effective information for platoon management while it is very sensitive to packet loss. Our study shows that communication is a critical factor in information exchange. Large packet loss can diminish values of data communication in platoon control.

This paper is only a first step in this direction. There are many un-resolved issues. We are currently investigating optimal information usage issues. Furthermore, we have only considered basic driving conditions: Straight lanes, dry surface conditions, good weather conditions, and no lane changes or platoon re-formation after vehicle departure or addition. All these issues are worth extensive studies.

REFERENCES

- [1] J.K. Hedrick, D. McMahon, D. Swaroop, Vehicle modeling and control for automated highway systems, PATH Research Report, UCB-ITS-PRR-93-24, 1993.
- [2] R. Rajamani, H.S. Tan, B. Law and W.B. Zhang, Demonstration of Integrated Lateral and Longitudinal Control for the Operation of Automated Vehicles in Platoons, *IEEE Transactions on Control Systems Technology*, Vol. 8, No. 4, pp. 695-708, July 2000.
- [3] S.B. Choi and J.K. Hedrick, Vehicle longitudinal control using an adaptive observer for automated highway systems, *Proc. of ACC*, Seattle, 1995.
- [4] C.Y. Liang and H. Peng, String stability analysis of adaptive cruise controlled vehicles, *ISME International Journal Series C*, Volume: 43, Issue: 3, pp. 671-677, 2000.
- [5] D. Swaroop and J.K. Hedrick, String Stability of Interconnected Systems, *IEEE Transactions on Automatic Control*, Vol. 41, No. 3, pp. 349-357, Mar. 1996.
- [6] H.C. Hsu and A. Liu, Kinematic design for platoon-lane-change maneuvers, *IEEE Transactions on Intelligent Transportation Systems*, Vol. 9, Issue 1, pp. 185-190, 2008
- [7] N. Alam and A.G. Dempster, Cooperative positioning for vehicular networks: facts and future, *IEEE Transactions on Intelligent Transportation Systems*, Vol. 14, Issue 4, pp. 1708-1717, 2013.
- [8] Le Yi Wang, Ali Syed, George Yin, Abhilash Pandya, Hongwei Zhang, Control of vehicle platoons for highway safety and efficient utility: Consensus with communications and vehicle dynamics, *Journal of Systems Science and Complexity*, accepted and to appear in 2013.
- [9] J. S. Freudenberg and R. H. Middleton, Feedback control performance over a noisy communication channel. *Proceedings of the 2008 Information Theory Workshop*, Porto, Portugal, pp. 232-236, May 2008.
- [10] R. Luck and A. Ray, Experimental verification of a delay compensation algorithm for integrated communication and control system. *International Journal of Control*, vol. 59, pp. 1357-1372, 1994.
- [11] L. Moreau, Stability of multiagent systems with time-dependent communication links, *IEEE Trans. Autom. Control*, vol. 50, no. 2, pp. 169-182, Feb. 2005.

- [12] G. N. Nair and R. J. Evans, Exponential stabilisability of finite-dimensional linear systems with limited data rates *Automatica*, 39 (2003) 585-593.
- [13] A. J. Rojas, J. H. Braslavsky, and R. H. Middleton, Fundamental Limitations in Control over a Communication Channel *Automatica* 44(2008), pp. 3147-3151.
- [14] Lijian Xu, Le Yi Wang, George Yin, Hongwei Zhang, Communication information structures and contents for enhanced safety of highway vehicle platoons, *IEEE Transaction of Vehicular Technology*, 2014, Digital Object Identifier: 10.1109/TVT.2014.2311384.
- [15] T. Richardson and R. Urbanke, *Modern Coding Theory*, Cambridge University Press, 2008.
- [16] Khalid Abdel Hafeez, Lian Zhao, Bobby Ma, and Jon W. Mark, Performance Analysis and Enhancement of the DSRC for VANETS Safety Applications, *IEEE Transaction of Vehicular Technology* VOL. 62, NO. 7, SEPTEMBER 2013.
- [17] Xiaoyan Yin, Xiaomin Ma, K. S. Trivedi, "An Interacting Stochastic Models Approach for the Performance Evaluation of DSRC Vehicular Safety Communication," *IEEE Transactions on Computers*, vol. 62, no. 5, pp. 873-885, 2013.
- [18] R.T. O'Brien, Vehicle lateral control for automated highway systems, *IEEE Transactions on Control Systems Technology*, Vol. 4-3, pp. 266 - 273, May 1996.
- [19] S. Sheikholeslam, C.A. Desoer, Longitudinal control of a platoon of vehicles with no communication of lead vehicle information: a system level study, *IEEE Transactions on Vehicular Technology*, Vol. 42-4, pp. 546 - 554, Nov 1993.
- [20] John Turner, *Automotive Sensors*, Momentum Press, 2009.
- [21] A. Lapidoth, The performance of convolutional codes on the block erasure channel using various finite interleaving techniques, *IEEE Trans. on Inform. Theory*, vol. 40, no. 5, pp. 1459-1473, Sept. 1994.
- [22] R. Knopp and P. Humblet, On coding for block fading channels, *IEEE Trans. on Inform. Theory*, vol. 46, no. 1, pp. 1643-1646, July 1999.
- [23] D. J. Costello, Jr., A. E. Pusane, S. Bates, and K. Sh. Zigangirov, A comparison between LDPC block and convolutional codes in *Proc. Information Theory and Applications Workshop*, San Diego, CA, USA, February 6-10, 2006.
- [24] A. Guillen, I. Fabregas, and G. Caire, Coded modulation in the block-fading channel: Code construction and coding theorems, *IEEE Trans. on Inform. Theory*, vol. 52, no. 1, Jan. 2006.
- [25] S. Dolinar, D. Divsalar, and F. Pollara Code Performance as a Function of Block Size, *TMO Progress Report*, pp. 42-133, 1998.
- [26] L.L. Peterson, B.S. Davie, *Computer Networks* (2nd Ed.), Morgan Kaufmann, San Francisco, CA, USA, 2000.
- [27] W. Stevens, *TCP/IP Illustrated* (Vol. 1, The Protocols), Addison-Wesley, Reading, MA, USA, 1994.
- [28] M.J. Neely and Eytan Modiano, Capacity and delay tradeoffs for Ad-Hoc mobile networks, *IEEE Tran. on Information Theory*, Vol. 51, No. 6, pp. 1917-1936 June 2005
- [29] A. Papoulis and S.U. Pillai, *Probability, Random Variables and Stochastic Processes*, 4th Edition, McGraw-Hill Europe, 2002.
- [30] R.G. Gallager, *Principles of Digital Communication*, 1st Edition, Cambridge University Press, 2008.
- [31] J.G. Proakis and M. Salehi, *Digital Communications*, 5th Edition, McGraw-Hill High Education, 2008.
- [32] D.H. McMahon, J.K. Hedrick, S.E. Shladover, Vehicle modelling and control for automated highway systems, *Proceedings of American Control Conference*, San Diego, CA, USA, pp. 297 - 303, May 23-25, 1990.
- [33] F. Bai, D.D. Stancil, H. Krishnan, Toward Understanding Characteristics of Dedicated Short Range Communications (DSRC) From a Perspective of Vehicular Network Engineers, *Proceedings of MobiCom10*, Chicago, IL, USA, pp. 329 - 340, September 20-24, 2010.
- [34] By John B. Kenney, Dedicated Short-Range Communications (DSRC) Standards in the United States, *Proceedings of the IEEE* Vol. 99, No. 7, July 2011.



Lijian Xu (S'11-M'14) received B.S. from University of Science and Technology Beijing China in 1998, M.S. from University of Central Florida in 2001, PhD from Wayne State University in 2014. He worked for AT&T, FL and Telus Communication, Canada as an engineer and engineering manager from 2001 to 2007. He is currently an Assistant Professor in Electrical and Computer Engineering Technology Department at Farmingdale State College, the State University of New York. His interests

are in the areas of network control system, digital wireless communication, consensus control, vehicle platoon and safety. He received The Best Paper Award from 2012 IEEE International Conference on Electro/Information Technology. He is a member of IEEE.



Le Yi Wang (S'85-M'89-SM'01-F'12) received the Ph.D. degree in electrical engineering from McGill University, Montreal, Canada, in 1990. Since 1990, he has been with Wayne State University, Detroit, Michigan, where he is currently a Professor in the Department of Electrical and Computer Engineering. His research interests are in the areas of complexity and information, system identification, robust control, H^∞ optimization, time-varying systems, adaptive systems, hybrid and nonlinear systems, information processing and learning, as well as medical, automotive, communications, power systems, and computer applications of control methodologies. He was a keynote speaker in several international conferences. He was an Associate Editor of the IEEE Transactions on Automatic Control and several other journals, and currently is an Associate Editor of the Journal of System Sciences and Complexity and Journal of Control Theory and Applications. He is a Fellow of IEEE.



George G. Yin (S'87-M'87-SM'96-F'02) received the B.S. degree in mathematics from the University of Delaware in 1983, M.S. in Electrical Engineering, and Ph.D. in Applied Mathematics from Brown University in 1987. He joined Wayne State University in 1987, and became a professor in 1996. His research interests include stochastic systems, applied stochastic processes and applications. He served on many technical committees; was the Co-chair of a couple of AMS-IMS-SIAM Summer Conferences, and the Co-chair of 2011 SIAM Control Conference.

He is or was an associate editor of many journals including SIAM Journal on Control and Optimization, *Automatica*, and *IEEE Transactions on Automatic Control*. He is a Fellow of IEEE.



Hongwei Zhang (S'01-M'07-SM'13/ACM S'01-M'07) received his B.S. and M.S. degrees in Computer Engineering from Chongqing University, China and his Ph.D. degree in Computer Science and Engineering from The Ohio State University. He is currently an associate professor of computer science at Wayne State University. His primary research interests lie in the modeling, algorithmic, and systems issues in wireless, vehicular, embedded, and sensor networks. His research has been an integral part of several NSF, DARPA projects such as the GENI WiMAX, ExoGENI, and ExScal projects. He is a recipient of the NSF CAREER Award. (URL: <http://www.cs.wayne.edu/hzhang>).